This manuscript has been authored by UT-Battelle, LLC under Contract No. DE-AC05-00OR22725 with the U.S. Department of Energy. The United States Government retains and the publisher, by accepting the article for publication, acknowledges that the United States Government retains a non-exclusive, paidup, irrevocable, world-wide license to publish or reproduce the published form of this manuscript, or allow others to do so, for United States Government purposes. The Department of Energy will provide public access to these results of federally sponsored research in accordance with the DOE Public Access Plan(http://energy.gov/downloads/doepublic-access-plan).

Spin-orbit driven magnetic insulating state with J_{eff}=1/2 character in a 4d oxide

S. Calder,[1,*] L. Li,[2] S. Okamoto,[3] Y. Choi,[4] R. Mukherjee,[2] D. Haskel,[4] and D. Mandrus[2,3]

[1] *Quantum Condensed Matter Division, Oak Ridge National Laboratory, Oak Ridge, Tennessee 37831, USA*
[2] *Department of Materials Science and Engineering, University of Tennessee, Knoxville, Tennessee 37996, USA*
[3] *Materials Science and Technology Division, Oak Ridge National Laboratory, Oak Ridge, Tennessee 37831, USA*
[4] *Advanced Photon Source, Argonne National Laboratory, Argonne, Illinois 60439, USA*

The unusual magnetic and electronic ground states of 5d iridates has been shown to be driven by intrinsically enhanced spin-orbit coupling (SOC). The influence of appreciable but reduced SOC in creating the manifested magnetic insulating states in 4d oxides is less clear, with one hurdle being the existence of such compounds. Here we present experimental and theoretical results on Sr_4RhO_6 that reveal SOC dominated behavior. Neutron measurements show the octahedra are both spatially separated and locally ideal, making the electronic ground state susceptible to alterations by SOC. Magnetic ordering is observed with a similar structure to an analogous J_{eff}=1/2 Mott iridate. We consider the underlying role of SOC in this rhodate with density functional theory and x-ray absorption spectroscopy and find a magnetic insulating ground state with J_{eff}=1/2 character.

The role of relativistic spin-orbit coupling (SOC) in creating the diverse behavior of transition metal oxides (TMOs) has largely been considered a perturbation. While this has proven a valid approximation when describing 3d based TMOs the recent intense interest in 5d systems has been driven specifically by the increased effects of SOC [1]. In 5d TMOs SOC competes with increased orbital overlap (altered bandwidth), reduced on-site Coulomb interactions (U) and enhanced crystal field splitting. The resulting behavior includes potential realizations of Weyl semi-metals [2, 3], Kitaev physics [4], topological insulators [5] and routes to unconventional superconductivity [6, 7].

One of the most dramatic and well studied manifestations of SOC in 5d systems was first observed in Sr_2IrO_4 with the creation of a magnetic J_{eff}=1/2 Mott insulating state [8, 9]. This ground state emerges in the Ir^{4+} ion with $5d^5$ occupancy due to the t_{2g} manifold, in the limit of cubic crystal field splitting, being split by SOC into a filled J_{eff}=3/2 band and a half filled J_{eff}=1/2 band, with even the reduced U in 5d systems being able to drive the opening of the insulating band gap via the Mott mechanism. Subsequent investigations on iridates have led to a growing list of candidate J_{eff}=1/2 magnetic materials [1]. Observations of J_{eff}=1/2 magnetic insulating behavior outside of the iridates is limited, with no known examples in 4d oxide based systems. Of particular interest in SOC enhanced magnetic states is the bond directional anisotropy of the J_{eff}=1/2 pseudo-spins and how alterations from the ideal case, such as tetragonal distortions or pressure-driven increase in bandwidth in Sr_2IrO_4 that causes mixing with J_{eff}=3/2 bands [10], influences the creation of exotic ground states.

The limit of a pure J_{eff}=1/2 state requires strong SOC and a cubic CEF environment. While 5d iridates fall into the strong SOC regime no current examples have a cubic environment. Nevertheless even with appreciable distortions the state is still realized in 5d systems, albeit with potential mixing in of the J_{eff}=3/2 bands [1]. The apparent robustness of the ground state indicates that the converse would be applicable; J_{eff}=1/2 behavior should be manifested in systems with near ideal octahedra even if the SOC is reduced from those found in 5d systems. However in 4d TMOs where single-ion SOC is of the order 0.15 eV [11, 12], compared to 0.5 eV for iridates, it is unclear whether J_{eff}=1/2-like Mott magnetism is manifested or whether they fall into the class of three Kramers states [12]. Outside oxides, examples of SOC enhanced behavior in 4d systems are limited to theoretical predictions in fluoride based paramagnetic Ir and Rh systems, characteristic behavior in the chloride α-$RuCl_3$ and non-magnetic semiconducting behavior in Li_2RhO_3 [13–16].

Here we show the first 4d based oxide compound to exhibit a magnetically ordered ground state with J_{eff}=1/2 character that offers a unique viewpoint on SOC enhanced behavior in general. The material we focus on, Sr_4RhO_6, hosts a Rh valence of 4+ ($4d^5$), the same valence as observed in the J_{eff}=1/2 iridates (Ir^{4+}, $5d^5$). Previous investigations of Sr_4RhO_6 have been extremely limited [17, 18]. Vente *et al.* observed an anomaly in the susceptibility around 8 K that suggested Sr_4RhO_6 was the first magnetically ordered Rh^{4+} compound, however no microscopic long range magnetic order has been measured.

Sr_4RhO_6 forms the same hexagonal space group $R\bar{3}c$ adopted by the J_{eff}=1/2 iridate Ca_4IrO_6. Although not having an O_h point group Ca_4IrO_6 was shown to reside close to the local cubic limit required for an unmixed J_{eff}=1/2 state [19]. We directly compare the properties and the role of SOC in these related 4d and 5d materials. Structurally we find the rhodate to reside even closer to the local cubic limit and, since it is isostructural to Ca_4IrO_6, has disconnected RhO_6 octahedra. This makes Sr_4RhO_6 an appealing candidate to look for J_{eff}=1/2 behavior since the expected narrow bands and strong $10Dq$ splitting will help to overcome the reduced SOC

in going from 5d to 4d systems. We consider these factors in contrast to Sr_2RhO_4, the rhodate analogue of Sr_2IrO_4, where the role of SOC is considered to be negligible [11]. Sr_2RhO_4 is a paramagnetic metal where the large bandwidth and distorted octahedra, as similarly found in Sr_2IrO_4, suppress the influence of SOC [11]. For Sr_4RhO_6 we present experimental neutron and x-ray results along with detailed density functional theory calculations that show SOC plays a crucial role in creating a ground state with $J_{\rm eff}$=1/2 character.

Polycrystalline samples of Sr_4RhO_6 were grown following a similar method described in the literature [18]. A stoichiometric mixture of high-purity $SrCO_3$, Rh_2O_3 were ground, pressed into pellets, and sintered in pure oxygen atmosphere at 900°C, 1000°C, and 1100°C with intermediate grindings. The reaction time for each temperature was 4 days. The sample was finally annealed at 1250°C for 15 days. The extensive heating is required to fully remove the Sr_2RhO_4 phase. A pellet was measured with a PPMS systems to probe the resistivity. Neutron powder diffraction (NPD) measurements were performed on a 5g sample on the diffractometer HB-2A at the High Flux Isotope Reactor (HFIR), ORNL. Measurements of the crystal structure were performed with a wavelength of λ=1.54 Å and measurements of the magnetic structure were performed with λ=2.41 Å. Temperature measurements at select 2Θ were performed with the HB-1A fixed incident energy triple-axis spectrometer with λ=2.36 Å. The branching ratio of the L-edges was measured with x-ray absorption near edge spectroscopy (XANES) at beamline 4-ID-D at the Advanced Photon Source (APS), Argonne National Laboratory. The fluorescence was collected with a detector placed upstream from the sample at 22° from the incoming beam. Measurement were performed on different areas of the powder-on-tape sample to ensure reproducibility. The DFT calculations were performed with the generalized gradient approximation and projector augmented wave (PAW) approach [20] as implemented in the Vienna ab initio simulation package (VASP) [21, 22]. For Rh and O standard potentials were used (Rh and O in the VASP distribution), and for Sr a potential in which semicore s and p states are treated as valence states is used (Srsv). The structural optimization was done using the doubled unit cell with the experimental lattice constants, a 2x2x2 k-point grid and an energy cutoff of 550 eV. Subsequently, the magnetic ground state was examined including the local U for the Rh d states to account for strong correlation effects [23] with U=2.5 and J_H=0.9 eV, where J_H is the Hund's coupling [24], as well as the SOC.

The structure of Sr_4RhO_6 has been previously established by laboratory x-ray measurements [18], however this technique is appreciably less sensitive to oxygen positions compared to neutrons. Given the importance of octahedral distortions in potentially controlling the mixing and subsequent $J_{\rm eff}$=1/2 character and emergent magnetic and electronic properties we performed NPD on the HB-2A diffractometer. The refined structure based on those in the literature remained stable to 3 K, within the magnetic regime. The sample was found to be of high quality with no Sr_2RhO_4 that forms in the intermediate growth phase and only ∼1.3% non-magnetic SrO impurity phase. The crystal structure obtained from NPD is shown in Fig. 1. The disconnected RhO_6 octahedra are evident, with no shared Rh-O bonds between octahedra. Moreover the ideal cubic nature of these octahedra are revealed with identical Rh-O bonds (2.0437(14) Å) and two O-Rh-O bond angles that deviate by a remarkably small amount of less than 0.1° from the ideal 90°. This contrasts with a deviation of ∼2° in Ca_4IrO_6 that is considered one of the closest $J_{\rm eff}$=1/2 with nearly regular octahedra [19]. Therefore structurally Sr_4RhO_6 appears well suited to host electronic and magnetic behavior that can be controlled by SOC.

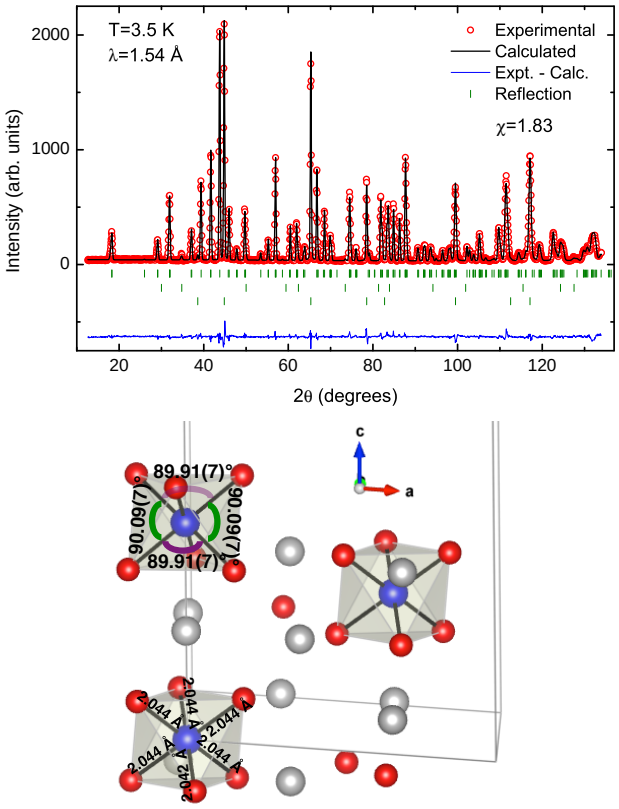

FIG. 1. Neutron powder diffraction measurements of the crystal structure of Sr_4RhO_6. The green tick marks correspond to Sr_4RhO_6, a small impurity phase of SrO and the Al sample can from top down, respectively. The bond angles and distances are shown between the O (red) and Rh (blue) ions in Sr_4RhO_6, revealing near ideal and isolated octahedra. The Sr ions are shown as grey spheres.

Before considering the electronic behavior further we address the significant question of whether Sr_4RhO_6 orders magnetically and the nature of the ground state.

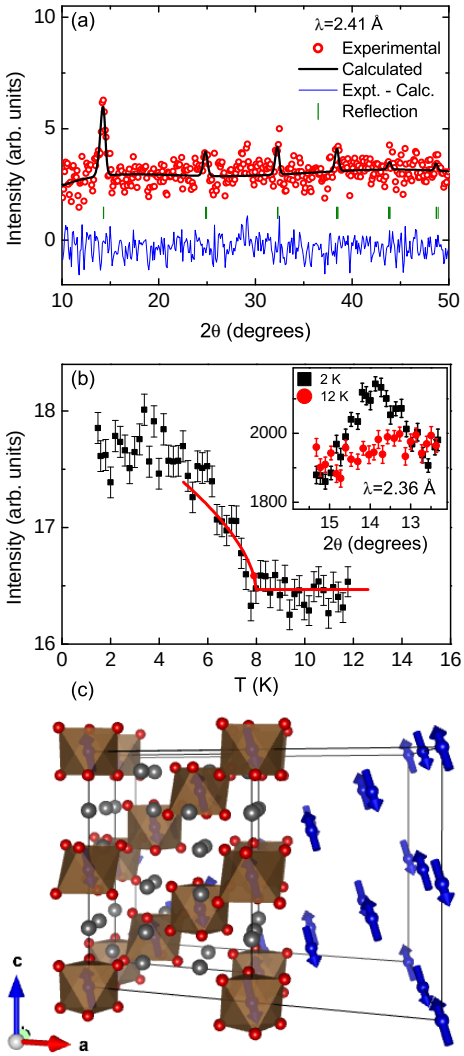

FIG. 2. (a) Difference of 15 K and 3 K neutron powder diffraction measurements. The fit is to the Γ_1 IR magnetic model. (b) The intensity of a magnetic reflection reveals long range magnetic ordering at 7.4(5) K in Sr_4RhO_6, the fit is to a power law. (c) The lowest energy Γ_1 magnetic ordering in Sr_4RhO_6.

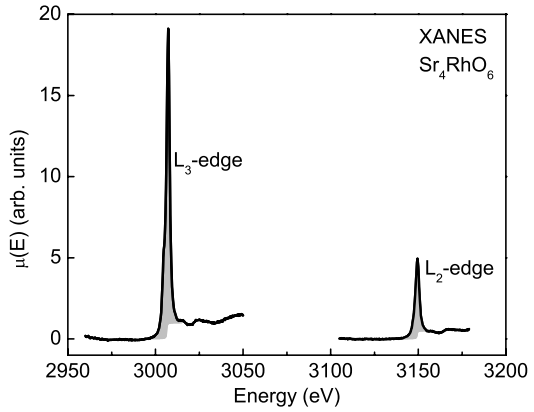

FIG. 3. Normalized and self-absorption corrected XANES measurements through the L_2 and L_3 edges in Sr_4RhO_6. The peak in the white line occurs at L_2=3149.0 eV and L_3=3007.12 eV. Measurements were performed at room temperature in fluorescence mode.

NPD has proven challenging for $J_{\rm eff}$=1/2 Ir-based compounds due to the combination of large neutron absorption, small moment size and pronounced magnetic form factor induced reduction in intensity with scattering angle. All of these factors are reduced when moving from Ir to Rh based systems and this allowed a successful NPD investigation with measurements performed through the reported anomaly in susceptibility to probe the microscopic magnetic structure. Comparing results at 15 K and 3 K shows the presence of extra intensity at low temperature at several reflection positions, see Fig. 2(a). All of the reflections are consistent with a propagation vector of $\mathbf{k}$=($\frac{1}{2}\frac{1}{2}$0) which corresponds to the same ordering vector as found in the iridate analogue Ca_4IrO_6 [19]. Following a representational analysis approach yields two possible irreducible representations (IR) that are both consistent with the observed NPD measurements [25]. These correspond to Γ_1 and Γ_3 in Kareps numbering scheme for the Rh ion at the 6*b* Wyckoff position, (0,0,0) site. Both IRs describe similar antiferromagnetic structures, with the distinction being either antiferromagnetic spins along the c-axis for Γ_1 or ferromagnetic chains along the c-axis for Γ_3. Given the non-first order nature of the transition (see Fig. 2(b)) we employ the simplification that only one IR describes the magnetic structure. To uncover the lowest energy magnetic ground state we performed DFT calculations for Sr_4RhO_6. It is found that the Γ_1 structure is lower in energy than the Γ_3 structure by 0.24eV per magnetic unit cell (0.01eV per Rh). Starting from parameters based on the refined NPD measurements we find Γ_1 with spins predominantly along the c-axis to be the lowest energy ground state. The results of magnetic refinements of the NPD for Γ_1 are shown in Fig. 2(a). The ordered magnetic moment from NPD measurements is 0.66(5)μ_B/Rh ion. Following the intensity of one of the magnetic reflections with temperature yields a magnetic ordering temperature of 7.4(5) K, as shown in Fig. 2(b). Contrasting with results on Ca_4IrO_6 [19] reveals both compounds adopt the same magnetic structure, although with slightly different canting from the c-axis and although the moment sizes are similar it is slightly larger in the rhodate. This would be expected in two compounds with similar magnetic ordering temperatures and underlying behavior, with the principle distinction being reduced itinerancy in the rhodate and subsequent increased local moment.

With the similarities between Sr_4RhO_6 and the $J_{\rm eff}$=1/2 iridate Ca_4IrO_6 in terms of the magnetic structure we now experimentally consider the role of SOC on Sr_4RhO_6. A useful probe in this regard for the iridates has proven to be x-ray absorption spectroscopy, where

the branching ratio (BR) of the L-edges provides evidence for the existence of enhanced SOC if the ratio deviates from the statistical value of 2 [26]. The BR is obtained by fitting the white lines from XANES measurements to a resolution broadened step function plus a lorentzian to obtain the integrated intensity, shown as the grey area in Fig. 3. The results reveal BR=3.6(2) for Sr_4RhO_6. The strong deviation from statistical indicates an appreciable role for SOC in the ground state. Indeed the values correspond closely to the BR for iridates that show strongly SOC enhanced behavior [26]. Similar XANES measurements on α-$RuCl_3$ revealed a BR of 3 that was presented as evidence for substantial SOC [14].

To further investigate the role of SOC we performed DFT calculations on Sr_4RhO_6 including the Γ_1 magnetic ground state. The results (Fig. 4(a)) show a t_{2g} manifold split into J_{eff}=1/2 and J_{eff}=3/2 dominated bands. The J_{eff}=1/2 states are higher in energy then J_{eff}=3/2 with the near-Fermi-level states given predominantly by the J_{eff}=1/2 states, and J_{eff}=3/2 fully filled. Therefore, while the splitting between J_{eff}=1/2 and J_{eff}=3/2 is not complete, as can be seen in the DOS, spectroscopically a pure J_{eff}=1/2 is realized because the scattering process is from the excited to the unoccupied states. Experimentally we probed the insulating nature with resistance measurements on a pressed pellet, see Fig. 4(b). These results are consistent with an insulating material and moreover the powder is dull, characteristic of an insulator. From DFT calculations an insulating gap of around 0.1 eV is observed. This insulating gap is reduced from that found in Ca_4IrO_6 from DFT of 0.6 eV. Moreover we find that unlike Ca_4IrO_6 the J_{eff}=1/2 and J_{eff}=3/2 bands are not fully separated. This mirrors the situation from DFT calculations in the paramagnetic fluoride based Ir and Rh systems predicted to both be J_{eff}=1/2 Mott insulators [13]. The mixed J_{eff} bands indicates that despite the essential ideal octahedra in Sr_4RhO_6 the intrinsic SOC is not large enough to fully split the t_{2g} manifold. This situation is analogous to several other candidate J_{eff}=1/2 materials where the opposite occurs: the J_{eff}=1/2 and J_{eff}=3/2 bands are mixed despite the large SOC due to appreciable non-cubic distortions.

Collectively our experimental and theoretical results reveal the behavior in Sr_4RhO_6 is strongly influenced by SOC. Qualitatively the results are very similar to the Rh based fluorides, however it is important to consider the differing effects of oxygen compared to fluorine. Specifically in oxides the hybridization is generally much stronger than fluorides. Consequently the band width of J_{eff}=1/2 dominated bands and J_{eff}=3/2 dominated bands are narrower in fluorides, of the order 0.1 eV compared to 0.5 eV in Sr_4RhO_6. Therefore while the degree of separation is stronger in the fluorides both show J_{eff}=1/2 character, although neither show fully separated J_{eff}=1/2 and J_{eff}=3/2 dominated bands. This leads to the question of whether an alternative approach is more appropriate in which both these fluoride and oxides system are best described by three Kramers states as considered for other rhodates [12]. However, as suggested in Ref. 12 the BR from XANES should distinguish between these cases and indeed this does so in Sr_4RhO_6.

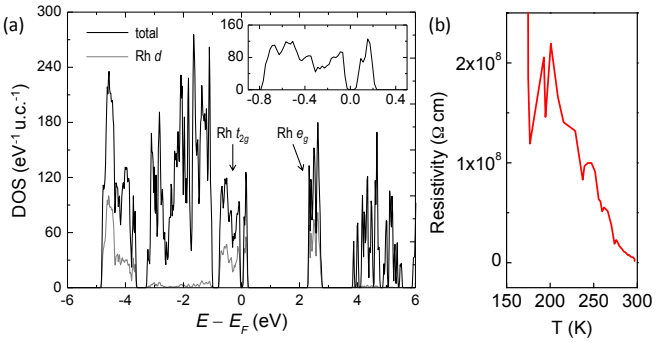

FIG. 4. (a) DFT calculations show the Γ_1 magnetic ordering is the lowest energy and insulating in Sr_4RhO_6. The area region around the Fermi energy is shown inset (b) The insulating nature was experimentally probed with resistivity measurements. The resistance increased with decreasing temperature, becoming immeasurably high below 160 K.

In conclusion, we have observed a rare occurrence of long range magnetic order in a rhodate compound. Moreover Sr_4RhO_6 is found to be an insulator leading to a consideration in terms of SOC enhanced behavior. Experimentally the magnetic ordering and insulating behavior are all analogous to the isostuctural J_{eff}=1/2 iridate Ca_4IrO_6. DFT calculations reveal J_{eff} character with mixed J_{eff}=1/2 and J_{eff}=3/2 dominated bands. Despite the mixing due to the reduced SOC in going from Ir to Rh the physical properties are strongly influenced by SOC. Therefore while this is the first 4d TMO to be shown to have J_{eff} character further investigations on oxides with similar spatially disconnected octahedra offer routes to uncovering analogous exotic properties as found in the iridates.

This research at ORNL's High Flux Isotope Reactor was sponsored by the Scientific User Facilities Division, Office of Basic Energy Sciences, U.S. Department of Energy. Use of the Advanced Photon Source, an Office of Science User Facility operated for the U.S. DOE Office of Science by Argonne National Laboratory, was supported by the U.S. DOE under Contract No. DE-AC02-06CH11357. S.O. is supported by the U.S. Department of Energy, Office of Science, Basic Energy Sciences,Materials Sciences and Engineering Division.

* caldersa@ornl.gov

[1] W. Witczak-Krempa, G. Chen, Y. B. Kim, and L. Balents, Annual Review of Condensed Matter Physics, **5**, 57 (2014).

[2] D. Pesin and L. Balents, Nature Phys., **6**, 376 (2010).
[3] X. Wan, A. M. Turner, A. Vishwanath, and S. Y. Savrasov, Phys. Rev. B, **83**, 205101 (2011).
[4] G. Jackeli and G. Khaliullin, Phys. Rev. Lett., **102**, 017205 (2009).
[5] Y. Chen, Y.-M. Lu, and H.-Y. Kee, Nat. Commun., **6**, 6593 (2015).
[6] J. Kim, D. Casa, M. H. Upton, T. Gog, Y.-J. Kim, J. F. Mitchell, M. van Veenendaal, M. Daghofer, J. van den Brink, G. Khaliullin, and B. J. Kim, Phys. Rev. Lett., **108**, 177003 (2012).
[7] Y. K. Kim, O. Krupin, J. D. Denlinger, A. Bostwick, E. Rotenberg, Q. Zhao, J. F. Mitchell, J. W. Allen, and B. J. Kim, Science, **345**, 187 (2014).
[8] B. J. Kim, H. Jin, S. J. Moon, J.-Y. Kim, B.-G. Park, C. S. Leem, J. Yu, T. W. Noh, C. Kim, S.-J. Oh, J.-H. Park, V. Durairaj, G. Cao, and E. Rotenberg, Phys. Rev. Lett., **101**, 076402 (2008).
[9] B. J. Kim, H. Ohsumi, T. Komesu, S. Sakai, T. Morita, H. Takagi, and T. Arima, Science, **323**, 1329 (2009).
[10] D. Haskel, G. Fabbris, M. Zhernenkov, P. P. Kong, C. Q. Jin, G. Cao, and M. van Veenendaal, Phys. Rev. Lett., **109**, 027204 (2012).
[11] T. F. Qi, O. B. Korneta, L. Li, K. Butrouna, V. S. Cao, X. Wan, P. Schlottmann, R. K. Kaul, and G. Cao, Phys. Rev. B, **86**, 125105 (2012).
[12] V. M. Katukuri, K. Roszeitis, V. Yushankhai, A. Mitrushchenkov, H. Stoll, M. van Veenendaal, P. Fulde, J. van den Brink, and L. Hozoi, Inorganic Chemistry, **53**, 4833 (2014).
[13] T. Birol and K. Haule, Phys. Rev. Lett., **114**, 096403 (2015).
[14] K. W. Plumb, J. P. Clancy, L. J. Sandilands, V. V. Shankar, Y. F. Hu, K. S. Burch, H.-Y. Kee, and Y.-J. Kim, Phys. Rev. B, **90**, 041112 (2014).
[15] A. Banerjee, C. Bridges, J.-Q. Yan, A. Aczel, L. Li, M. Stone, G. Granroth, M. Lumsden, Y. Yiu, J. Knolle, D. Kovrizhin, S. Bhattacharjee, R. Moessner, D. Tennant, D. Mandrus, and S. Nagler, arXiv:1504.08037 (2015).
[16] Y. Luo, C. Cao, B. Si, Y. Li, J. Bao, H. Guo, X. Yang, C. Shen, C. Feng, J. Dai, G. Cao, and Z.-a. Xu, Phys. Rev. B, **87**, 161121 (2013).
[17] J. J. Randall, Jnr and L. Katz, Acta Crystallographica, **12**, 519 (1959).
[18] J. F. Vente, J. K. Lear, and P. D. Battle, J. Mater. Chem., **5**, 1785 (1995).
[19] S. Calder, G.-X. Cao, S. Okamoto, J. W. Kim, V. R. Cooper, Z. Gai, B. C. Sales, M. D. Lumsden, D. Mandrus, and A. D. Christianson, Phys. Rev. B, **89**, 081104 (2014).
[20] P. E. Blochl, G. Kresse, and D. Joubert, Phys. Rev. B, **59**, 17953 (1994).
[21] G. Kresse and D. Joubert, Phys. Rev. B, **59**, 1758 (1999).
[22] G. Kresse and J. Furthmller, Phys. Rev. B, **54**, 111169 (1996).
[23] G. I. Liechtenstein, V. I. Anisimov, and J. Zaanen, Phys. Rev. B, **52**, R5467 (1995).
[24] G.-Q. Liu, V. N. Antonov, O. Jepsen, and O. K. Andersen., Phys. Rev. Lett., **101**, 026408 (2008).
[25] A. Wills, Physica B, **276**, 680 (2000).
[26] M. A. Laguna-Marco, D. Haskel, N. Souza-Neto, J. C. Lang, V. V. Krishnamurthy, S. Chikara, G. Cao, and M. van Veenendaal, Phys. Rev. Lett., **105**, 216407 (2010).